INSTITUTE OF PHYSICS PUBLISHING PLASMA PHYSICS AND CONTROLLED FUSION

Plasma Phys. Control. Fusion **45** (2003) A17–A30 PII: S0741-3335(03)69360-7

# Key issues in plasma–wall interactions for ITER: a European approach

**V Philipps**[1], **J Roth**[2] **and A Loarte**[3]

[1] Institut für Plasmaphysik, Forschungszentrum Jülich, Association EURATOM, 52425 Jülich, Germany
[2] Max-Planck-Institut für Plasmaphysik, IPP-EURATOM Association, Boltzmannstraße 2, 85748 Garching, Germany
[3] EFDA Close Support Unit, Boltzmannstraße 2, 85748 Garching, Germany

Received 11 July 2003
Published 10 November 2003
Online at stacks.iop.org/PPCF/45/A17

**Abstract**

The first burning fusion plasma experiment based on the tokamak principle, international tokamak experimental reactor (ITER) is now ready for construction. Based on the continuous progress of many years of fusion research, the design relies upon a large and robust set of experimental data. The focus of present day fusion research is therefore shifting towards the issues of ITER plasma operation and machine availability. The latter is governed mainly by plasma–wall interaction issues, in particular the lifetime of plasma-facing components and long-term tritium retention. To coordinate the research activities in this area a task force for plasma–wall interaction (EU-PWI-TF) has been initiated by the European fusion research programme under EFDA. This contribution describes the experimental database in these areas and outlines the task force strategy and further research that will be needed to address the critical issues.

## 1. Introduction

The international tokamak experimental reactor (ITER) has been finally designed and can be constructed. This is the collaborative result of decades of fusion research from many experimental magnetic fusion devices world-wide, which has resulted in a large and robust database. The design meets the scientific and technological objectives within appropriate margins. These are:

- a long-pulse (∼8 min) burning fusion plasma at an energy amplification factor, $Q$, of at least 10 for a plasma current of 15 MA,
- the capability to investigate steady-state plasma operation, with parameters that allow $Q = 5$ and 'hybrid' scenarios with pulse lengths of the order of 30 min,
- integration and investigation of fusion technology relevant for the first commercial-type fusion reactor (DEMO).

  

Various questions, however, remain open, for which the confidence is less robust and/or that cannot be addressed sufficiently in present experiments. They are key areas of ongoing research, but final answers might only be given by ITER itself as a physics experiment. These issues are largely related to plasma–wall interaction processes connected principally with the extended duty cycle and increase in the plasma stored energy. The constraints are:

- to achieve technically acceptable conditions for the heat and power exhaust ($10\,\mathrm{MW\,m^{-2}}$ continuous on divertor target plates),
- to achieve a sufficient lifetime of the plasma-facing components (PFCs; $>3000$ ITER shots). This goal is largely related to the control of transient heat loads during edge localized modes (ELMs) and to disruptions. Sublimation or melt layer limit of the target materials must be avoided,
- to stay below the long-term tritium inventory limit, which is set by safety considerations to 350 g T.

In the past, efforts in divertor and plasma edge physics research have been directed principally towards the development of scenarios for power and particle exhaust. They are available now and are based on high-density divertor operation, which leads to plasma detachment, reducing the peak divertor power loads by radiation, charge exchange and recombination processes [1, 2]. This will not be discussed further here, but any plasma scenario or new wall material choices must be compatible with these conditions.

The issues of PFCs lifetime and long-term tritium retention are priority areas of the EU-PWI-TF. These processes are controlled by material erosion and the succeeding short- and long-range migration. Extrapolation from present day devices having a full carbon wall clearly shows that the long-term tritium retention in ITER would soon exceed the T-retention limit (350 g). This means that only an unacceptably limited number of pulses in a D–T mixture would be allowed in a full graphitic wall environment. However, ITER will have different wall materials, with Be as the material in the main chamber ($700\,\mathrm{m^2}$), tungsten in the upper regions of the divertor and the dome region ($70\,\mathrm{m^2}$) and carbon fibre composite (CFC) tiles on a relatively small area ($50\,\mathrm{m^2}$) on the high-flux regions in the lower divertor (figure 1). This will change the carbon erosion and redeposition behaviour and most probably relax the T-retention problem compared with a full carbon device. The challenge is to predict the lifetime and T-retention under these conditions quantitatively in the absence of tokamak experiments with an ITER-like material composition.

An improved physics understanding of the underlying processes is therefore needed to predict the fuel retention and lifetime. This is also the basis for development of techniques to mitigate or control the T-retention, e.g. by means of carbon traps, temperature tailoring or sophisticated geometry. In parallel, more work must be done to develop ITER-compatible methods for the removal of T from PFC or co-deposited layers. Finally, one has to consider the situation that the long-term T-retention in ITER will be unacceptably high if carbonaceous wall materials are used. To be prepared for this situation, a full-metal first-wall scenario must therefore be developed.

A coordinated European research activity has been established (EU task force on plasma–wall interaction) to provide improved information regarding the lifetime of the ITER target plates and the rate of tritium inventory build-up and to suggest improvements, including material changes, that could be implemented at an appropriate stage. The purpose of this contribution is to summarize the present experience and data in these key areas and to outline the strategy of the EU-PWI-TF.

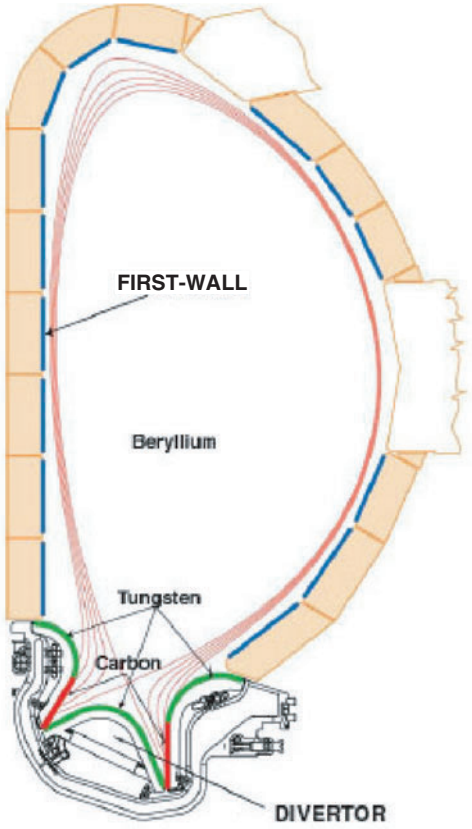


**Figure 1.** Cut-away showing the layout of PFCs in ITER with different armour materials.

## 2. Observations on fuel (tritium) retention in present devices

The retention of hydrogen in graphite by implantation and the formation of amorphous hydrogen-rich carbon layers upon impact of carbon atoms or ions together with hydrogen species has well known since long and has also been observed in fusion devices [2–4]. However, the severity of the problem for the next-step device was only revealed after first tritium experiments in TFTR [5] and JET [6]. About 3 and 36 g of T were injected in TFTR and JET, respectively, from which large amounts (30–40%) were retained on a short timescale (days) in the machine (as shown in figure 2) upper part. Large amounts of fuel are also observed to be retained in first-wall surfaces at the end of single discharges, e.g. in JET, Tore Supra and other machines (e.g. [4]). Despite various cleaning mechanisms (not discussed here), about 13% and 10% of the T remained in TFTR and JET, respectively. These observations are well in line with findings from devices operating in hydrogen or deuterium, e.g. such as TEXTOR. In TEXTOR the amount of long-term D retention has been assessed by adding up the amounts of D found in carbon layers deposited at various locations compared with the cumulative D input over the plasma operation time (about half a year), yielding a very similar retained fraction of 8% [7]. Extrapolating such values to ITER (fuelling rate 200 Pa $m^3$ $s^{-1}$) the T safety limit of 350 g would be reached in <50 plasma discharges. Thereafter, cleaning procedures must be applied to recover the fuel for further tritium plasma operation.

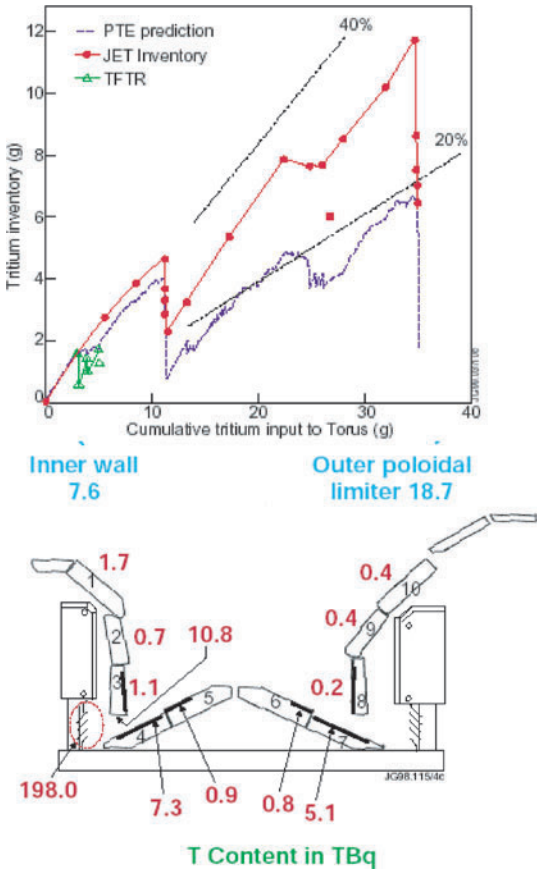


**Figure 2.** Upper: cumulative retention of tritium inside JET and TFTR after the tritium plasma operation campaigns [5, 6]. Lower: tritium distribution in the JET tiles after cleaning procedures measured by post mortem surface analysis [54].

It is found that the majority of the long-term retained fuel is stored in carbon layers built up by redeposition of eroded carbon along with the hydrogenic fuel (co-deposits) formed at different locations in the machine [7, 9–11]. On erosion-dominated graphite areas, the fuel retention is restricted to implantation in a shallow surface layer, enhanced due to adsorption onto rough surfaces of CFC tiles, saturating at few $10^{17}$ H cm$^{-2}$ [8]. This extrapolates to 5 g T for the first-wall area of ITER (if made from graphite) and is tolerable. Co-deposited C- layers, however, contain hydrogen fractions up to 1 : 1 H/C, depending on temperature and impact particle energy, with the layer growth continuing for as long as erosion occurs. Layers are formed not only on many locations of the plasma-facing wall tiles but also on areas with no direct plasma ion impact ('remote areas'). It turns out that understanding tritium retention requires understanding the erosion of carbon and local and global transport inside the device or to remote areas. The main goal of the EU-PWI-TF work is to initiate coordinated analysis and experiments to understand these processes in detail.

## 3. Location and strength of impurity sources

In the past, priority has always been assigned to measurement of divertor impurity sources and their screening, with a lower emphasis on wall sources. Relatively recent post mortem analysis

of wall tiles has revealed, however, that the material deposition found in the divertor originates predominantly from main chamber erosion. Strong evidence for this has been presented from AUG [9] and JET [10]. In JET strong deposition is found at the inner target plates, whilst erosion/deposition in the outer target is balanced, pointing to the wall as the main source of material [10]. In addition, Be is evaporated routinely onto the JET main wall surfaces with no line of sight to the divertor target surfaces. Nevertheless, Be is found mainly on the plasma-facing sides of the inner divertor [13]. In AUG, both divertor targets are deposition-dominated, requiring a net material source in the main chamber [11]. Previous AUG operation with the W-divertor showed little change of the main plasma carbon content and a strong C deposition in the inner divertor, indicating that erosion of carbon in the main chamber is the source of the carbon deposited in the divertor and found in the main plasma [14]. In DIII-D, recent spectroscopic analysis of the divertor and main chamber C-sources has revealed a major contribution of carbon from the main chamber to the total carbon discharge content [15].

Quantification of main chamber impurity sources is difficult due to the large areas and the restricted number of spectroscopic lines of sight. In JET, a combination of main chamber spectroscopy, methane injection screening experiments and edge modelling indicates a carbon source strength of about $3 \times 10^{20}\,\mathrm{C\,s^{-1}}$ and $3.2 \times 10^{20}\,\mathrm{C\,s^{-1}}$, respectively, in the operational campaigns in which the MKIIA and MKGB divertors were installed (see figure 3). This amounts to a total carbon wall source of about 390 g C and 440 g C, respectively [16]. The averaged Be wall source in JET is about ten times smaller, reflecting the inhomogeneous Be coverage of the wall and the fast erosion of the thin Be layer [16]. These C-sources must be compared with the carbon deposition in the JET divertors, where a total amount of 1000 g in MKIIA and 400–500 g in MKBG were found. Although analysis to consolidate the latter value is ongoing, the values are in surprisingly fair agreement with the carbon sources from the main chamber. The carbon influx from the main chamber in AUG has been evaluated by spectroscopy and is about $1 \times 10^{20}\,\mathrm{C\,s^{-1}}$ [17]. The C influx in JET and AUG therefore appears to scale roughly as the first-wall area ($\approx$50 m$^2$ and $\approx$200 m$^2$, respectively).

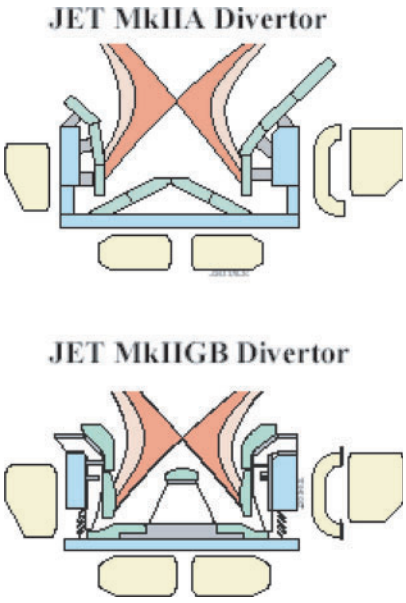


**Figure 3.** Schematic view of the JET MKIIA and MKGB configurations.

Present data cannot directly discriminate between the contribution of ion- and neutral-induced erosion of main chamber surfaces and of the fraction of chemical and physical erosion. Lowering the wall temperature in JET from 320°C to 220°C did not affect the carbon flux from the wall (based on C III spectroscopy), indicating either a significant contribution of physical sputtering or a weak dependence of chemical erosion in this temperature range [18]. Comparison of discharges in D and He showed a strongly reduced carbon influx in He, indicating that ion-induced physical sputtering cannot play the dominant role [19]. These questions need to be addressed further in order to better predict the main chamber Be erosion in ITER. It is also important to identify the main chamber locations from which the impurities are released. In AUG, covering the inner wall with tungsten did not significantly decrease the plasma carbon content. It resulted in a partial coverage of the inner wall with carbon. This strongly suggests the outer wall (graphite guard limiters) to be the dominant carbon source [20].

The radial decrease of the magnetic field from the inner to the outer first-wall allows carbon sources to be discriminated from the high- and low-field side spectroscopically. In AUG this method revealed a larger C-recycling source at the inner wall, coated with the tungsten layer [17]. Obviously the C recycles many times on the inner wall while it is initially released on the outer wall. In JET, similar measurements show no clear preference of carbon released from the inner or outer wall. This is consistent with $H_\alpha$ tomography of inner and outer wall recycling fluxes at JET, indicating about equal contributions from both [21]. An enhanced transport mechanism in the outer scrape-off layer (SOL), based on ballooning-like blobby transport, which predicts plasma interaction mainly on the outer wall areas [22], has recently been the subject of much discussion. This is confirmed qualitatively by camera observations and probe measurements. The strength of this contribution to the main chamber plasma interaction is yet to be quantified.

Connected with this main chamber recycling is the question of what is the fraction of main chamber interaction during and in-between ELMS. At the divertor targets the ELMs carry typically about 30% of the power, but this fraction might be larger for a plasma–wall interaction in the main chamber. Evidence for this has been observed in JET and elsewhere [23, 24], but again a quantification is still missing. It should be mentioned that the ELM-induced rise in the target temperature in the JET divertor is already close to the carbon sublimation limit in high-performance type I ELM discharges (low ELM frequency), but the main chamber observations, which are restricted to CCD observations, do not indicate such high temperatures. This indicates that ELMs in the divertor are more severe than in the main chamber. If this is confirmed, it would ease the problem of the narrow power margins for the target plates, but more direct main chamber fast IR thermography measurements are necessary to address this question more precisely.

In general, there is insufficient knowledge regarding main chamber plasma–wall interaction processes. Efforts should focus on

- identifying locations and strengths of main chamber impurity sources,
- identifying the contribution of ion- and neutral-induced erosion and, for C, the fraction of physical and chemically induced erosion,
- identifying the fraction of erosion between ELMs and during ELMs and analysing the dependence of ELM-induced erosion on the ELM type and parameters.

## 4. Long-range material migration

With the ion grad $B$ drift directed downwards, all major tokamaks observe that the material eroded in the main chamber flows into the inner divertor, which inturn becomes a

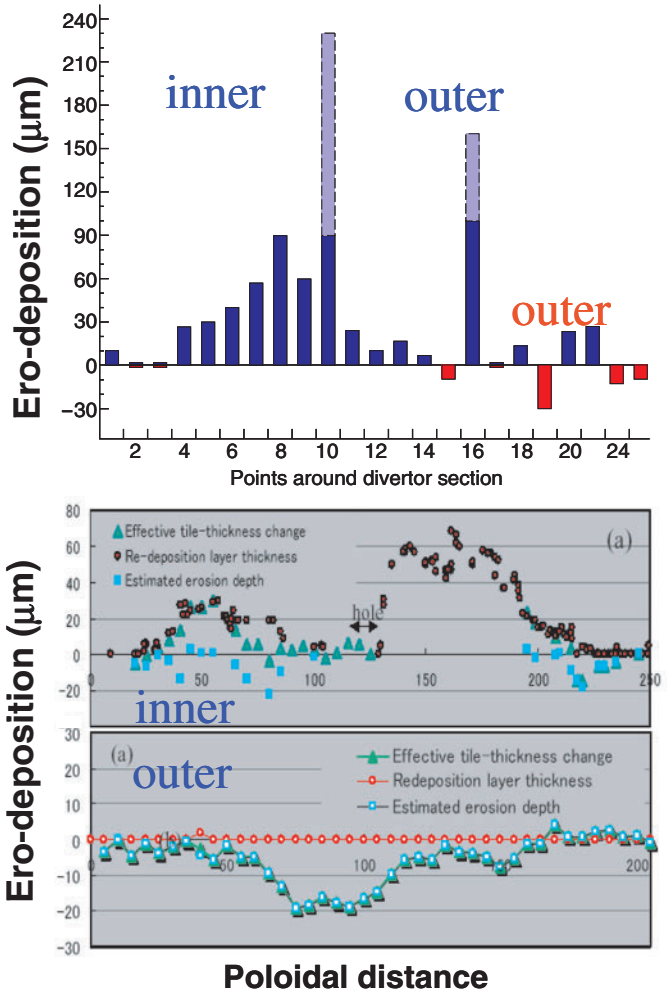


**Figure 4.** Erosion deposition pattern for the JET MKIIA divertor and JT60 divertor. Data have been obtained by post mortem thickness analysis and are for about 5700 and 4300 discharges for JET and JT60U, respectively [10, 12].

deposition-dominated area [25]. As an example, figure 4 shows the erosion deposition pattern in the more closed JET MKIIA divertor and for the case of the more open JT-60U divertor. This behaviour has been confirmed recently in JET by $^{13}$C-marked methane injection from the top of the machine. Subsequent surface analysis of wall and divertor tiles showed that the majority of the $^{13}$C is found in the inner divertor and, to a lesser extent, on the main chamber tiles, whereas no $^{13}$C was detected in the outer divertor [26]. The behaviour in the outer divertor differs from machine to machine and can depend on divertor geometry (JET [25], AUG [27]) or plasma conditions (DIII).

The larger surface area of the low-field side SOL, which favours energy flow to the outer divertor, cannot explain alone the in–out asymmetry of material deposition observed in present devices. It is largely determined by preferential flows in the plasma SOL towards the inner divertor (with the grad($B$) $\times$ $B$ drift direction towards the X-point). These flows reach Mach numbers as high as 0.5 in JET at the top of the machine, significantly larger than

the classical flow speed predicted from $E \times B$ and grad $B \times B$ drifts (Mach number of about 0.1) [28]. In JET it has been shown that localized main chamber recycling cannot produce such flows and an explanation of their nature is still being sought [29]. Promising attempts have been made to explain a component of the flows by radial fluctuations [30]. Observations in JT-60U show a flow through the private flux region from the outer to the inner divertor [31]. This is confirmed by modelling and is of importance for the material transport discussed here. Two issues must therefore be addressed.

- Explaining the flows in existing devices. This is required for the prediction of SOL flows in ITER, which themselves influence the Be deposition of the inner and outer graphite divertor tiles and thus the physical and chemical erosion of the underlying graphite.
- Analysing possible flows in the private flux region. Such flows may short-circuit the outer and inner divertors, which would strongly affect the material transport.

## 5. Short-range material transport inside the divertor

Experimental data on material transport in the inner divertor are available mainly for carbon. JET provides important data on transport of Be, which is evaporated in the main chamber, and additional measurements will soon be available on tungsten transport in the AUG divertor [32]. In devices that apply boronization, boron transport can also be analysed and compared with that of carbon. This approach has not been used extensively so far but is strongly recommended.

In the JET MKIIA divertor, the influx ratio of C to Be into the divertor is measured to be about 12 [16], but the layers formed on the plasma-facing side of the tiles are Be-rich, with a ratio C/Be of typically 0.3–1 [13]. This shows that carbon does not remain in the layers and undergoes further erosion-induced transport, whilst Be adheres to the surface. The majority ($>$90%) of the carbon flowing into the divertor is found on shadowed areas of horizontal tile 4 (see figure 2) and on the water-cooled louvres at the entrance of the pump duct. This can be seen, e.g. for the MKIIA divertor case, on the T-distribution inside the divertor, measured by post mortem analysis, as shown in the lower part of figure 2. A large part of the material has fallen down in the divertor floor in the form of flakes [10]. In the JET gas box divertor (MKIIGB) the carbon deposition in the divertor is very similar ($\approx$500 g in total compared with 1000 g in MKIIA), but the majority of the carbon is now on tile 4 and on the septum, whereas the Be is mostly deposited on tiles 1 and 3. The amount of carbon that enters the louvre entrance area has been determined by *in situ* quartz micro-balance techniques (QMB) [33] and sticking monitors [34]. Both diagnostics show that the material flow to this area is largely reduced (at least a factor of ten) compared with the previous MKIIA. In addition, the QMB data show that the amount of carbon deposited at the QMB location increases when the distance of the strike point on the vertical tiles to the louvre entrance decreases (the QMB is then inside the private flux region). Most deposition is found with the strike point on the horizontal tile and consequently with the QMB in the SOL (figure 5). This was the favoured configuration in the previous MKIIA divertor configuration and may explain to a large extent the strong carbon deposition on the louvres.

In AUG and JT-60U, divertor tile analysis is ongoing, but the present data indicate the majority of carbon is deposited on the plasma-facing side of the divertor tiles, as with the JET MKIIGB observations. In AUG, layer growth is also observed in the subdivertor region [11], but the carbon deposition on the plasma-facing sides is stronger. Sticking monitors mounted in the inner divertor region of the JET gas box divertor [34] show that the majority ($>$90%) of particles have high sticking probabilities and only a small fraction has low sticking. A similar conclusion must be drawn from observations of carbon deposition into shadowed areas of the

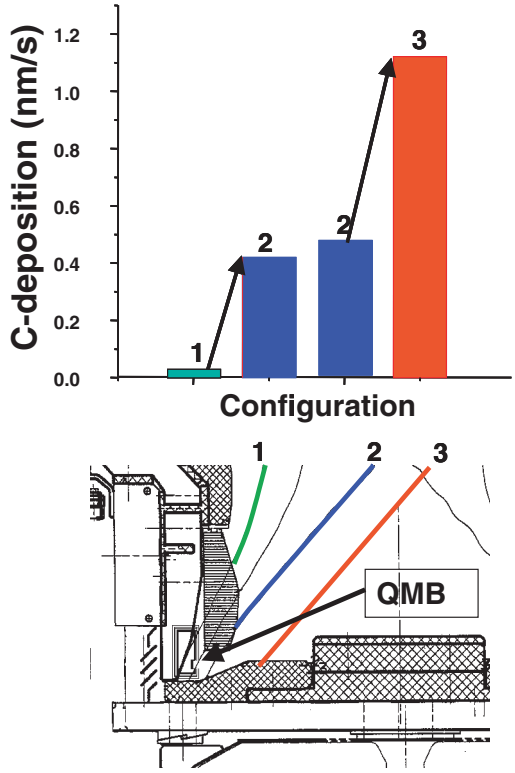


**Figure 5.** Carbon deposition on the QMB for identical discharges with different plasma configuration. The lower part shows the different positions of the strike point in the inner divertor.

limiters in TEXTOR (drill holes) [7]. Also, boron is not transported in TEXTOR towards remote areas, e.g. the TEXTOR limiter pump ducts, while carbon films are formed on those areas, albeit representing only a small part of the total carbon transport [35]. The high sticking probability of the majority of the carbon species allows only a small fraction of the carbon species to reach the pump ducts before being deposited. Elements that show no chemical erosion, like Be in JET, B in TEXTOR or W in AUG, do not show long-range transport at all.

The outer divertor in JET shows almost no clear erosion or deposition (except on a narrow band on the horizontal tile near the edge of the lower vertical tile) and behaves thus in a favourable manner: carbon is eroded but locally re-deposited and not transported for larger distances. The particle fluence towards the outer divertor in the JET MKIIGB series ($1.5 \times 10^{27}$ $D^+$) would produce a total erosion of about 600 $\mu$m, suggesting effective local re-deposition of the eroded carbon. In contrast, the inner and outer divertor targets in AUG are now deposition-dominated, indicating influx from sources in the main chamber [36]. Here also, important questions await further clarification.

- The physics of carbon migration to remote areas requires further study: is this due to preferential chemical erosion of C or due to thermal decomposition of 'soft' mixed C/Be films? Are transient heating events by ELMs important for the carbon transport?
- Is the divertor transport of the carbon arriving from the main chamber different from that carbon which is eroded from the divertor target itself? This question is important for ITER, where the C flux from the main chamber is absent.

- What is the reason for the difference in transport behaviour of carbon in the JET outer and inner divertors: is this due to differences in plasma parameters or to the missing carbon flux from the main chamber to the outer target?

## 6. Modelling of impurity transport

Development of impurity transport codes validated thoroughly against experimental results is the final tool to predict material transport and fuel retention in ITER. Existing packages are fluid and Monte Carlo edge codes solving the transport equations of particles and energy in the plasma edge (B2-Eirene [38], Edge2D [39]) and local impurity transport codes following the trajectories of impurities in a limited volume near the target plates (WBC-code [37], ERO-code [40]). The edge codes provide the input of particles and the local plasma parameters for local transport codes. Comparison of transport code results with various experimental observations in TEXTOR [41] and JET [42] show that the modelled re-deposition and transport pattern of C does not agree with experimental observations. In JET the modelled amount of carbon migrating to the louvres is about a factor of ten lower than that observed experimentally, and the local re-deposition of $^{13}CH_4$ on the TEXTOR limiters is about a factor of 50 too small compared with experiment. In these calculations 'standard' assumptions concerning erosion yields were used, such as physical sputtering according to Yamamura formulas [43], 2% chemical erosion and sticking probabilities of re-deposited species according to the TRIM kinetic reflection model [44]. Much better agreement can be achieved if the erosion yields are enhanced and the sticking probabilities decreased. However, high sticking probabilities [7, 34] are observed in experiments and the present assumption is thus that the re-erosion of a re-deposited carbon by the background plasma is much larger compared with a carbon atom in a graphitic surface plane. Also, the sticking of low-energy hydrocarbon radicals returning to the surface has been lowered in accordance with new molecular dynamics calculations [45] and experimental investigations using thermal radical beams. In this area more effort is required to

- improve the input database, such as chemical erosion yields, atomic data for the break-up of hydrocarbon species or sticking probabilities of hydrocarbon radicals and carbon atoms,
- benchmark transport models in dedicated experiments of impurity transport under different plasma conditions.

## 7. Other key PWI questions for ITER

It is a challenge to predict the effect of Be deposition on the erosion behaviour of the graphite target tiles in ITER, in particular in the presence of transient heat loads by ELMs or disruptions. A large Be impurity flow towards the inner divertor is predicted, although more quantitative estimates are required, which will turn the inner divertor into a deposition-dominated zone. The influence of beryllium deposition on the carbon erosion has been studied in the PISCES plasma simulator in cooperation with the EU-PWI programme [46]. Complete suppression of the carbon chemical erosion due to Be coverage is observed, confirming the hope that carbon transport in the inner divertor of ITER can be reduced significantly. However, the ELM power deposition in ITER will only be marginally below the sublimation limit of graphite and may ablate the protective Be layer regularly, exposing the carbon surface again. On the other hand, the formation of Be–C compounds that might survive these temperature excursions may also occur under these conditions. Predictions for the outer target are more difficult since the Be flux to the divertor is unclear and physical re-sputtering of Be is higher.

The T-retention in the Be layers must be also assessed. In [16] a Be deposition of about 60 g/discharge is predicted. This requires a T/Be ratio $<10^{-2}$ in order to stay below the T-limit of 350 g for 1000 discharges. Pure Be retains only minor amounts of T, while incorporation of carbon or oxygen will enhance the retention [47].

Another key area of research is to explore all possible techniques to remove the fuel from fusion devices. This is *a priori* easier on areas directly facing the plasma (where we expect the Be layers), compared with shadowed or remote areas without a direct line of sight to plasma particles and power impact. On plasma-facing surfaces the plasma impact itself can be used to remove the retained T by isotope exchange or plasma-induced surface heating. However, this would require enough flexibility of the plasma configuration in the divertor. On those areas, external heating by lamps or lasers might also be possible. These techniques cannot be used on remote areas for which no clear scenario presently exists except mechanical tools or the use of gaseous, chemical treatments by active oxygen or ozone [48, 49]. These techniques must be compatible with plasma operation and need research in present tokamaks. The main important issues that should be addressed here are:

- to evaluate the influence of Be deposition on carbon physical and chemical erosion,
- to evaluate the thermal stability of Be/C layers during transient heat loads,
- to explore all possible methods to remove fuel from PFCs and from co-deposits and to demonstrate their tokamak applicability and plasma compatibility.

## 8. Development of a scenario without graphite wall components

Graphite is no option for DEMO due to the neutron-induced material damage. In addition, the T-retention limit with graphitic components in ITER is unlikely to be fulfilled. Thus a coherent metal wall scenario must be developed in parallel with the present first-wall material option. This implies that the following must be demonstrated:

- The compatibility of a tungsten divertor with the plasma operation scenarios foreseen for ITER, particularly the non-inductive current drive and the improved confinement scenarios.
- The compatibility of a tungsten divertor with the power exhaust requirement allowing a maximum steady-state power flux of $10\,\mathrm{MW\,m^{-2}}$. In particular, detachment physics in the absence of carbon as a main radiator must be investigated. Beryllium radiation will replace this, but additional impurity seeding might be necessary, possibly triggering tungsten impurity release and plasma tungsten contamination.
- An acceptable lifetime of the tungsten target in presence of melt layer erosion by transient heat loads during ELMs or disruptions.

The main task of the EU-PWI-TF is to concentrate on the last issue, while for a coherent approach the first two issues are also necessary. For ELMs, the tolerable energy loss limit is slightly higher for tungsten than for graphite. The carbon sublimation limit for graphite is $40\,\mathrm{MW\,m^{-2}\,s^{-0.5}}$, while for tungsten the melt layer limit is $60\,\mathrm{MW\,m^{-2}\,s^{-0.5}}$ [50]. The main advantage of CFC is that it does not melt if a few ELMs exceed this limit, whilst tungsten will show melt layer erosion. Tungsten surfaces may also develop hot spots on the edges of the molten zones, resulting in a reduced power handling capability. The constraints on plasma operation from the viewpoint of the tolerable ELM energy loss are similar for W and C, about 2–3% of stored plasma energy, but the advantage of graphite is that it can tolerate larger deviations of the actual ELM power loss from the averaged value [50]. This is shown in figure 6. Nevertheless, the main driver for CFC in the strike point divertor region is the possible melt layer loss of W in disruptions. In the ITER physics basis report [1] the melt layer

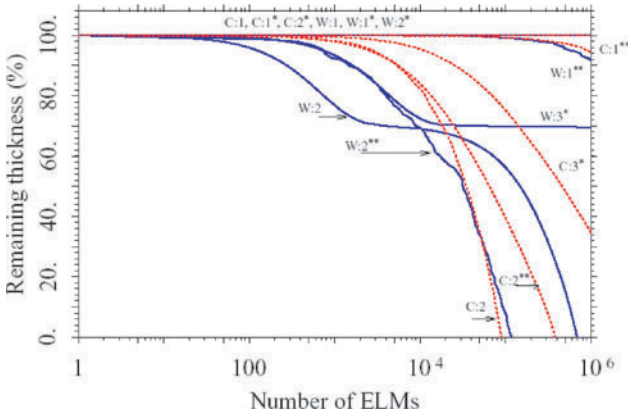


**Figure 6.** Remaining thickness vs number of ELMs for a CFC target (· · · · · ·) and W target (——). The different curves refer to a fraction of the pedestal energy (∼105 MJ) loss during type I ELMs of (1) 0.05, (2) 0.1 and (3) 0.15. Cases refer to an inter-ELM heat flux of 5 MW m$^{-2}$ and ELMs with a triangular waveform with ramp-up and ramp-down phases lasting 0.5 ms each. Cases (*) refer to a more inclined target. Cases (**) refer to erosion analyses done with a statistical evaluation of ELM parameters for a more inclined target (from [49]).

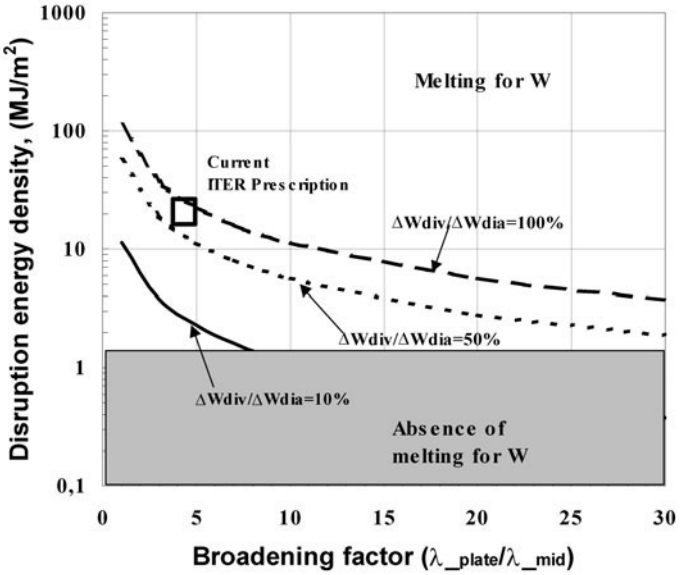


**Figure 7.** Parameter space for melting of W in ITER depending on disruption energy loss, disruption power deposition profile and fraction of energy arriving in the divertor. Also shown is the present ITER assumption [49].

erosion of W in disruptions is estimated based on the assumptions that (i) the plasma stored energy is lost towards the divertor, (ii) the power decay length of a disruption is three times broader than for normal plasma operation and (iii) half the melt layer is lost by splashing. These assumptions result in loss of tungsten of about 50 $\mu$m per disruption, which reduces the lifetime of a W target to unacceptably low values. Figure 7 shows the parameter space of disruption energy loss, power deposition profile and fraction of energy arriving in the divertor

together with the parameter space for which melting of tungsten is avoided [50]. Recent observations in AUG, DIII and JET [51–53] show that only a fraction of the thermal energy is deposited in the divertor and the power is spread over much larger areas than previously assumed. It is evident that the power loss by disruptions is a key issue of the EU-PWI-TF. Research will focus on

- the energy flux to the divertor and main chamber, the spatial and time evolution during thermal quench and the dependence on disruption type,
- the development of disruption mitigation techniques relevant for ITER.

## 9. Summary

Long-term tritium retention is the most critical issue for ITER. Predictions for ITER need improvements based on dedicated understanding in present devices. An integrated approach and understanding is necessary of

- where and how impurities are produced in the main chamber?
- how they are transported towards the divertor?
- how the material is transported inside the divertor, in particular to remote areas?

Transport models on long- and short-range impurity migration have to be further developed and benchmarked against dedicated experiments under various conditions.

Techniques to control *in situ* tritium retention and to remove tritium from PFCs and co-deposited layers on remote areas must be developed. Their tokamak applicability and compatibility must be addressed in present tokamak research.

It may turn out that the use of graphite in ITER is incompatible with the T-retention limit. This requires a coordinated effort to develop a tungsten divertor scenario and the use of metal in the main chamber. The scenario has to be compatible with the main requirements of plasma operation, power exhaust and target lifetime. The EU-PWI-TF work will focus on characterization of the disruption power deposition and the development of disruption mitigation techniques.

More tokamak experiments are needed to investigate the issues discussed in this contribution under ITER-like wall material conditions or under conditions avoiding the use of graphite in the main chamber.

## References

[1] ITER Physics Basis Editors 1999 *Nucl. Fusion* **39** 2137
[2] Federici G *et al* 2001 *Nucl. Fusion* **41** 1967
[3] Rubel M *et al* 2003 *Phys. Scr.* T **103** 20–4
[4] Loarer T *et al* 2003 *30th Conf. on Controlled Fusion and Plasma Physics (St Petersburg, Russia, 7–11 July 2003)*
[5] Skinner C *et al* 1997 *J. Nucl. Mater.* **241–243** 214
[6] Andrew P, Brennan P D and Coad J P 1999 *Fusion Eng. Des.* **47** 233–45
[7] Wienhold P *et al* 2003 *J. Nucl. Mater.* **313–316** 311–20
[8] Maier H *et al* 1999 *J. Nucl. Mater* **266–269** 1003
[9] Roth J and Janeschitz G 1989 *Nucl. Fusion* **29** 915
[10] Coad P *et al* 2003 *J. Nucl. Mater.* **313–316** 419–23
[11] Rohde V *et al* 2003 *J. Nucl. Mater.* **313–316** 337–41
[12] Gotoh Y *et al* 2003 *J. Nucl. Mater.* **313–316** 370–6
[13] Rubel M *et al* 2003 *J. Nucl. Mater.* **313–316** 321–6
[14] Neu R *et al* 1996 *Plasma Phys. Control. Fusion* **38** A165
[15] Whyte D G *et al* 2001 *J. Nucl. Mater.* **290–293** 356–61

[16] Matthews G *et al* 2003 *30th Conf. on Controlled Fusion and Plasma Physics (St Petersburg, Russia, 7–11 July 2003)*
[17] Pütterich T *et al* 2003 *Plasma Phys. Control. Fusion* **45** 1873–92
Pugno R *et al* 2001 *J. Nucl. Mater.* **290–293** 308
[18] Pospieszczyk A *et al* 1999 *Phys. Scr.* T **81** 48
[19] Pitts R *et al* 2003 *J. Nucl. Mater.* **313–316** 777–86
[20] Neu R *et al* 2003 *J. Nucl. Mater.* **3313–3316** 116–26
[21] Lipschultz B *et al* 2003 *30th Conf. on Controlled Fusion and Plasma Physics (Russia, Petersburg, 7–11 July 2003)*
[22] Sarazin Y *et al* 2003 *J. Nucl. Mater.* **313–316** 796–803
[23] Fundamenski W *et al* 2003 *30th Conf. on Controlled Fusion and Plasma Physics (Russia, Petersburg, 7–11 July 2003)*
[24] Counsell G *et al* 2002 *15th PSI Conf. (Gifu, 2002)*
[25] Whyte D G *et al* 1999 *Nucl. Fusion* **39** 1025
[26] Likonen J *et al* 2003 *Fusion Eng. Des.* **66–68** 219–24
[27] Neu R, Kallenbach A and Krieger K 2003 *Fusion Sci. Technol.* at press
[28] Erents S K *et al* 2000 *Plasma Phys. Control. Fusion* **42** 905
[29] Chankin A, Corrigan G and Erents S K 2001 *J. Nucl. Mater.* **290–293** 518
[30] Hidalgo C *et al* this conference
[31] Asakura N *et al* 2000 *Phys. Rev. Lett.* **84** 3093
[32] Geier A *et al* 2003 *J. Nucl. Mater.* **313–316** 1216 and this conference
[33] Esser H G *et al* 2003 *Fusion Eng. Des.* **66–68** 855–60
[34] Mayer M *et al* this conference
[35] von Seggern J *et al* 2003 *J. Nucl. Mater.* **3313–3316** 439–43
Mayer M *et al* 2003 *J. Nucl. Mater.* **313–316** 429
[36] Maier H *et al* 1999 *EPS Maastricht*
[37] Brooks J 1990 *Phys. Fluids* B **2** 1858
Brooks J N *et al* 2003 *J. Nucl. Mater.* **313–316** 424
[38] Reiter D *et al* 1992 *J. Nucl. Mater.* **196–198** 80
[39] Simonini R *et al* 1994 *Contrib. Plasma Phys.* **34** 368
[40] Kirschner A, Philipps V, Winter J and Kögler U *Nucl. Fusion* **40** 989
[41] Kirschner A *et al* 2001 *J. Nucl. Mater.* **290–293** 238–44
[42] Kirschner A *et al* 2003 *Plasma. Phys. Control. Fusion* **45** 309
[43] Yamamura Y, Itikawa Y and Itoh N 1983 *Rep. IPPJAM-26* NIFS, Nagoya
[44] Eckstein W 1991 *Computer Simulation of Ion Solid Interaction* (Berlin: Springer)
[45] Alman A, Ruzic D N and Brooks J N 2003 *J. Nucl. Mater.* **313–316** 182–6
[46] Doerner R *et al* 2003 *Phys. Scr.* at press
[47] Anderl R A *et al* 1999 *J. Nucl. Mater.* **273** 1–26
[48] Moormann R *et al* 2000 *Fusion Eng. Des.* **49–50** 295–301
[49] Philipps V *et al* 1999 *J. Nucl. Mater.* **266–269** 386–91
[50] Federici G 2003 *Plasma Phys. Control. Fusion* **45** 1523–47
[51] Pautasso G *et al* 2002 *Nucl. Fusion* **42** 100
[52] Andrew P *et al* 2003 *J. Nucl. Mater.* **313–316** 135–9
[53] Whyte D G *et al* 2002 *IAEA Conf. (Lyon)*
[54] Coad J P *et al* 2001 *J. Nucl.* **290–293** 224